Constraints on Compact Star Radii and the Equation of State From Gravitational Waves, Pulsars and Supernovae

J. M. Lattimer

Department of Physics & Astronomy

Stony Brook University

U.S. Department of Energy Office of Science

Collaborators: E. Brown (MSU), C. Drischler (TU Darmstadt), K. Hebeler (OSU), D. Page (UNAM), C.J. Pethick (NORDITA), M. Prakash (Ohio U), A. Steiner (UTK), A. Schwenk (TU Darmstadt)

Compact Stars and Gravitational Waves
Yukawa Institute of Theoretical Physics
1 November, 2016

Outline

- The Dense Matter EOS and Neutron Star Structure
  - General Causality, Maximum Mass and GR Limits
  - Neutron Matter and the Nuclear Symmetry Energy
  - Theoretical and Experimental Constraints on the Symmetry Energy
- Extrapolating to High Densities with Piecewise Polytropes
- Radius Constraints Without Radius Observations
- Universal Relations
- Observational Constraints on Radii
  - Photospheric Radius Expansion Bursts
  - Thermal Emission from Quiescent Binary Sources
  - Ultra-Relativistic Neutron Star Binaries
  - Neutron Star Mergers
  - Supernova Neutrinos
  - X-ray Timing of Bursters and Pulsars
  - Effects of Systematic Uncertainties

Dany Page
UNAM

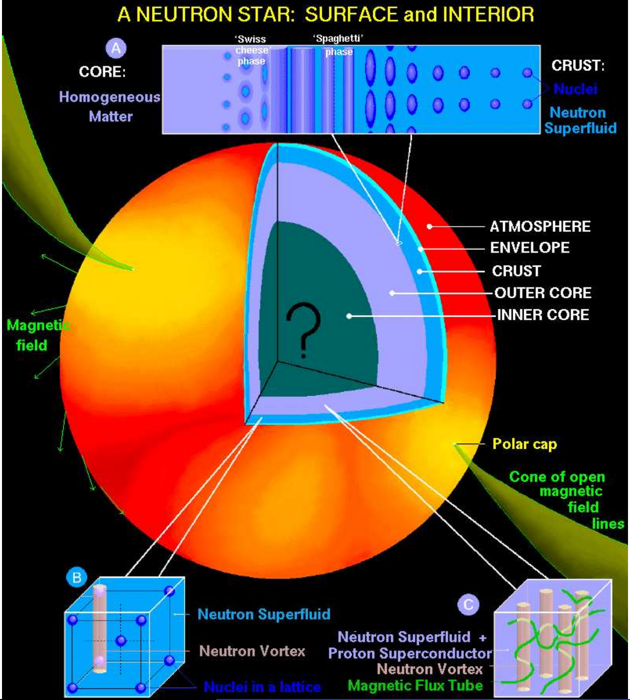

Neutron Star Structure

Tolman-Oppenheimer-Volkov equations

$$\frac{dp}{dr} = -\frac{G}{c^4}\frac{(mc^2+4\pi pr^3)(\varepsilon+p)}{r(r-2Gm/c^2)}$$

$$\frac{dm}{dr} = 4\pi\frac{\varepsilon}{c^2}r^2$$

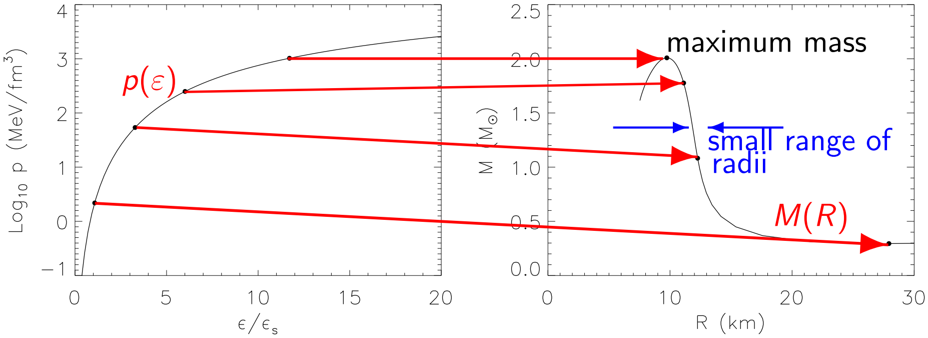

Equation of State ← Observations

Extremal Properties of Neutron Stars

- The most compact and massive configurations occur when the low-density equation of state is "soft" and the high-density equation of state is "stiff" (Koranda, Stergioulas & Friedman 1997).

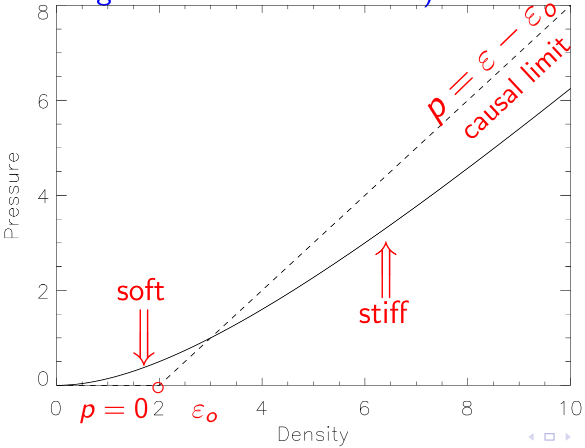

ε_o is the only EOS parameter

The TOV solutions scale with ε_o

Causality + GR Limits and the Maximum Mass

A lower limit to the maximum mass sets a lower limit to the radius for a given mass.

Similarly, a precision upper limit to R sets an upper limit to the maximum mass.

$R_{1.4} > 8.15 M_\odot$ if $M_{max} \geq 2.01 M_\odot$.

$M_{max} < 2.4 M_\odot$ if $R < 10.3$ km.

$M - R$ curves for minimally compact EOS

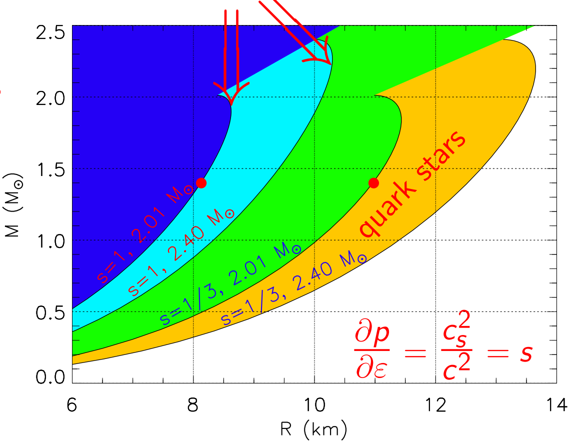

If quark matter exists in the interior, the minimum radii are substantially larger.

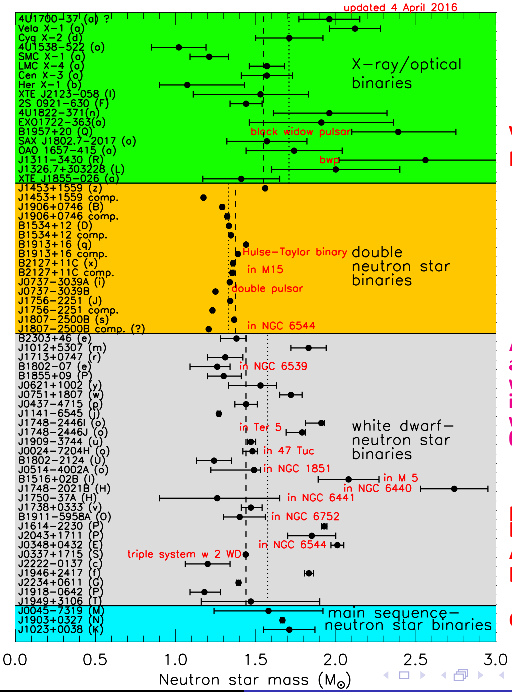

vanKerkwijk 2010

Romani et al. 2012

Although simple average mass of w.d. companions is 0.23 $M_\odot$ larger, weighted average is 0.04 $M_\odot$ smaller

Demorest et al. 2010
Fonseca et al. 2016

Antoniadis et al. 2013

Barr et al. 2016

Champion et al. 2008

Mass-Radius Diagram and Theoretical Constraints

GR:

$R > 2GM/c^2$

$P < \infty$:

$R > (9/4)GM/c^2$

causality:

$R \gtrsim 2.9GM/c^2$

— normal NS

— SQS

— $R_\infty = \dfrac{R}{\sqrt{1-2GM/Rc^2}}$

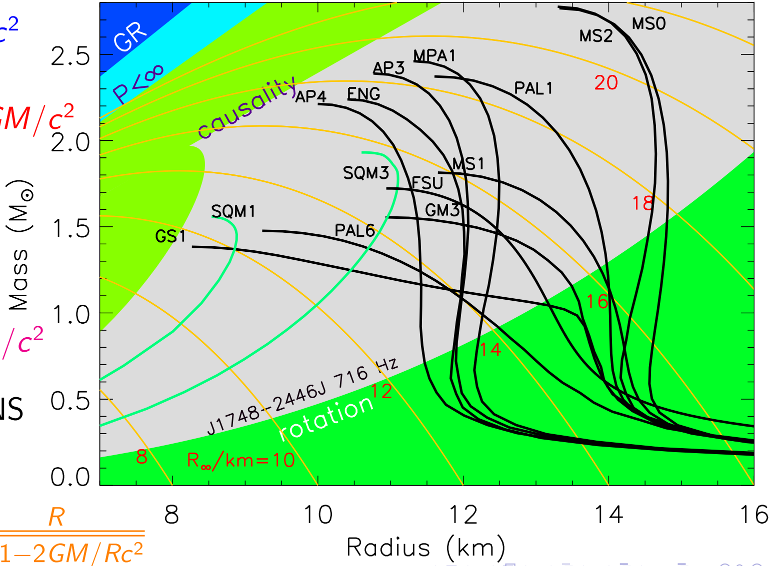

Neutron Star Radii and Nuclear Symmetry Energy

- Radii are highly correlated with the neutron star matter pressure around $(1-2)n_s \simeq (0.16-0.32)\ \mathrm{fm}^{-3}$. (Lattimer & Prakash 2001)
- Neutron star matter is nearly purely neutrons, $x \sim 0.04$.
- Nuclear symmetry energy

$$S(n) \equiv E(n, x=0) - E(n, 1/2)$$

$$E(n,x) \simeq E(n,1/2) + S_2(n)(1-2x)^2 + \ldots$$

$$S(n) \simeq S_2(n) \simeq S_v + \frac{L}{3}\frac{n-n_s}{n_s} + \frac{K_{sym}}{18}\left(\frac{n-n_s}{n_s}\right)^2 \ldots$$

- $S_v \sim 32$ MeV; $L \sim 50$ MeV from nuclear systematics.
- Neutron matter energy and pressure at n_s:

$$E(n_s,0) \simeq S_v + E(n_s,1/2) = S_v - B \sim 16\ \mathrm{MeV}$$

$$p(n_s,0) = \left(n^2\frac{\partial E(n,0)}{\partial n}\right)_{n_s} \simeq \frac{Ln_s}{3} \sim 2.7\ \mathrm{MeV\ fm}^{-3}$$

Theoretical Neutron Matter Calculations

Nuclei provide information for matter up to n_s.

Theoretical studies, beginning from fitting low-energy neutron scattering data and few-body calculations of light nuclei, can probe higher densities.

- Auxiliary Field Diffusion Quantum Monte Carlo (Gandolfi & Carlson)
- Chiral Lagrangian Expansion (Drischler, Hebeler & Schwenk; Sammarruca et al.)

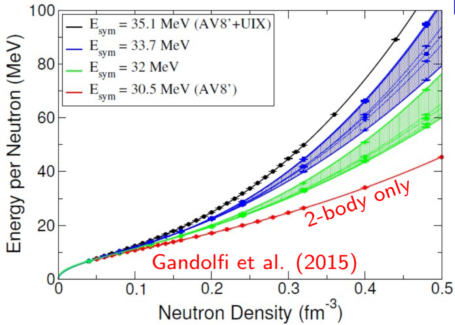

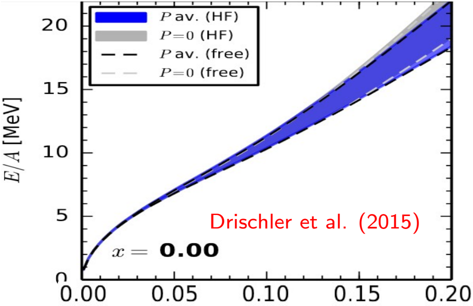

- Chiral Lagrangian calculations of neutron-rich and symmetric matter (Drischler, Hebeler & Schwenk 2016) strongly suggest that the quadratic interpolation

$$E(n,x) = E(n,1/2) + S_2(n)(1-2x)^2$$

is accurate to within ± 0.5 MeV for $0 < n \lesssim (5/4)n_s$ for $x << 1$. In other words

$$S(n) \simeq S_2(n) \equiv \frac{1}{8}\left(\frac{\partial^2 E(n,x)}{\partial x^2}\right)_{x=1/2},$$

and

$$E(n_s,0) = S_v + B, \qquad p(n_s,0) = Ln_s/3.$$

- Experimental constraints on saturation properties (Brown & Schwenk 2014; Kortelainen et al. 2014, Piekarewicz 2010)

$$B = -15.9 \pm 0.4 \text{ MeV}, \qquad n_s = 0.164 \pm 0.007 \text{fm}^{-3},$$

$$K = 240 \pm 20 \text{ MeV}.$$

Unitary Gas Bounds

The assumption that the energy of neutron matter should be larger than the unitary gas, *i.e.*, fermions interacting via pairwise short-range s-wave interaction with an infinite scattering length, which shows a universal behavior, produces strong constraints on the symmetry parameters S_v and L (Kolomeitsev et al. 2016).

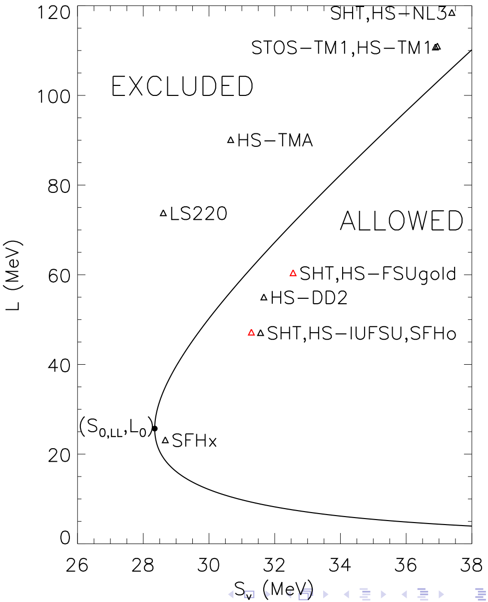

Nuclear Experimental Constraints

The liquid droplet model is a useful frame of reference. Its symmetry parameters S_v and S_s are related to S_v and L:

$$\frac{S_s}{S_v} \simeq \frac{aL}{r_o S_v}\left[1+\frac{L}{6S_v}-\frac{K_{sym}}{12L}+\ldots\right].$$

- Symmetry contribution to the binding energy:

$$E_{sym} \simeq S_v A I^2 \left[1+\frac{S_s}{S_v A^{1/3}}\right]^{-1}.$$

- Giant Dipole Resonance (dipole polarizability)

$$\alpha_D \simeq \frac{AR^2}{20 S_v}\left(1+\frac{5}{3}\frac{S_s}{S_v A^{1/3}}\right).$$

- Neutron Skin Thickness

$$r_{np} \simeq \sqrt{\frac{3}{5}}\frac{2r_o I}{3}\frac{S_s}{S_v}\left(1+\frac{S_s}{S_v A^{1/3}}\right)^{-1}\left(1+\frac{10}{3}\frac{S_s}{S_v A^{1/3}}\right).$$

Theoretical and Experimental Constraints

H Chiral Lagrangian

G: Quantum Monte Carlo

$S_v - L$ constraints from Hebeler et al. (2012)

Experimental constraints are compatible with unitary gas bounds.

Neutron matter constraints are compatible with experimental constraints.

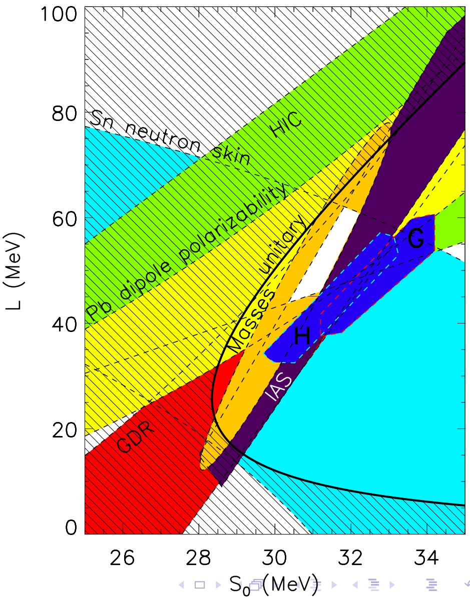

Neutron Star Crusts

The evidence is overwhelming that neutron stars have hadronic crusts.

- Neutron star cooling, both long term (ages up to millions of years) and transient (days to years), supports the existence of $\sim 0.5 - 1$ km thick crusts with masses $\sim 0.02 - 0.05 M_\odot$.
- Pulsar glitches are best explained by n $^1S_0$ superfluidity, largely confined to the crust, $\Delta I/I \sim 0.01 - 0.05$.

The crust EOS, dominated by relativistic degenerate electrons, is very well understood.

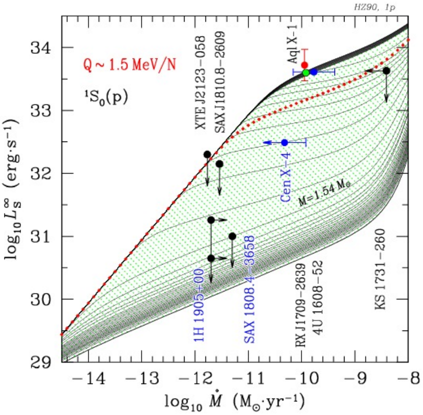

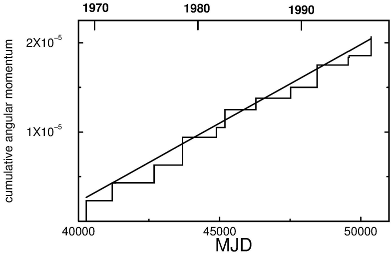

Piecewise Polytropes

Crust EOS is known: $n < n_0 = 0.4n_s$.

Read, Lackey, Owen & Friedman (2009) found high-density EOS can be modeled as piecewise polytropes with 3 segments.

They found universal break points ($n_1 \simeq 1.85n_s$, $n_2 \simeq 3.7n_s$) optimized fits to a wide family of modeled EOSs.

For $n_0 < n < n_1$, assume neutron matter EOS. Arbitrarily choose $n_3 = 7.4n_s$.

For a given p_1 (or Γ_1):
$0 < \Gamma_2 < \Gamma_{2c}$ or $p_1 < p_2 < p_{2c}$.
$0 < \Gamma_3 < \Gamma_{3c}$ or $p_2 < p_3 < p_{3c}$.

Minimum values of p_2, p_3 set by M_{max}; maximum values set by causality.

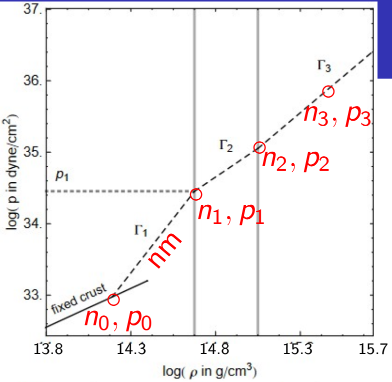

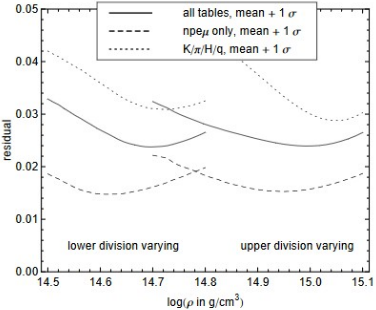

Causality

Even if the EOS becomes acausal at high densities, it may not do so in a neutron star.
We automatically reject parameter sets which become acausal for $n \leq n_2$. We consider two model subsets:

- Model A: Reject parameter sets that violate causality in the maximum mass star.
- Model B: If a parameter set results in causality being violated within the maximum mass star, extrapolate to higher densities assuming $c_s = c$.

Maximum Mass and Causality Constraints

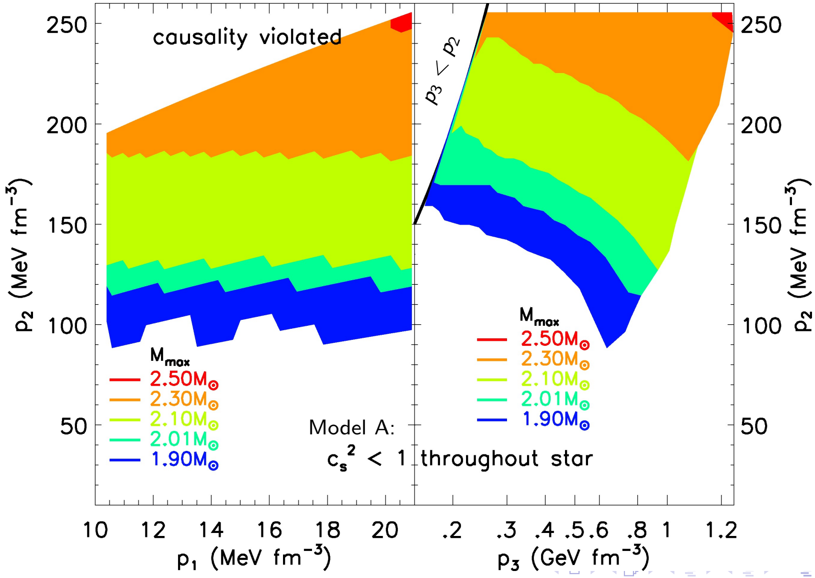

Radius - p_1 Correlation

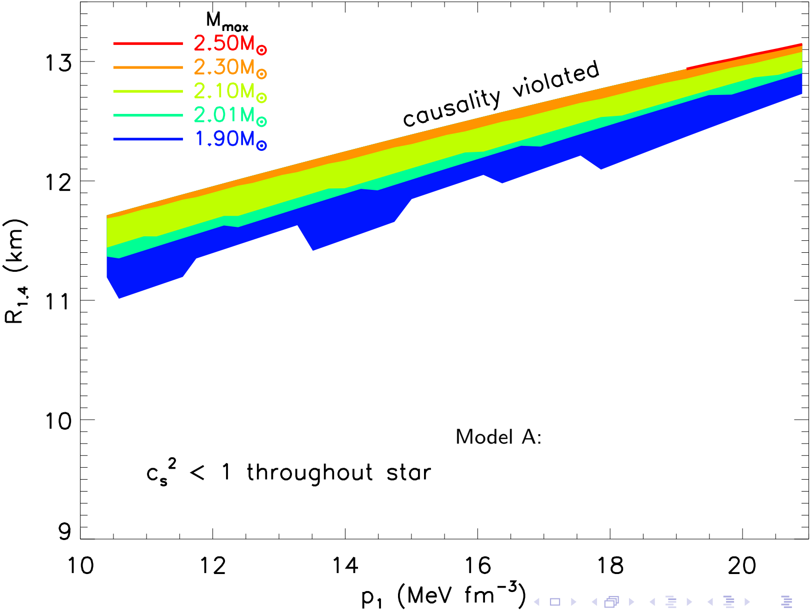

Mass-Radius Constraints from Causality

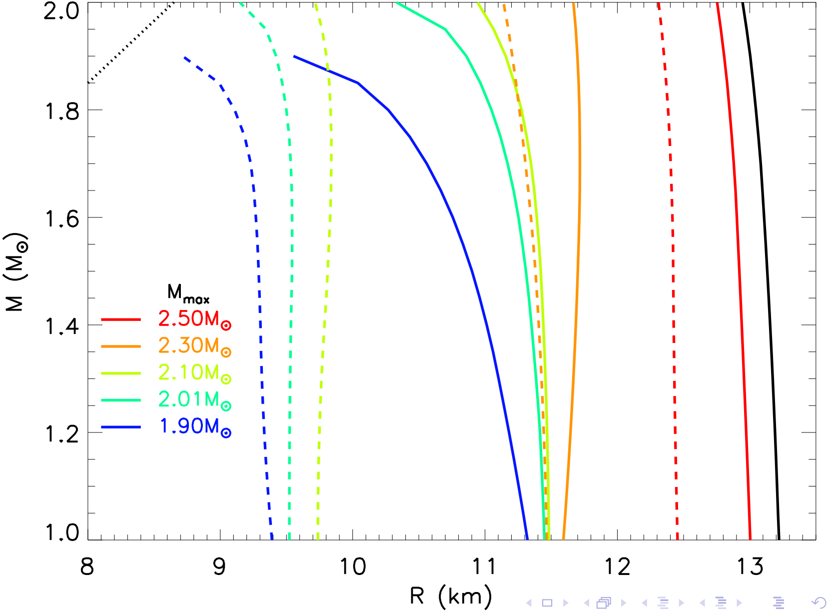

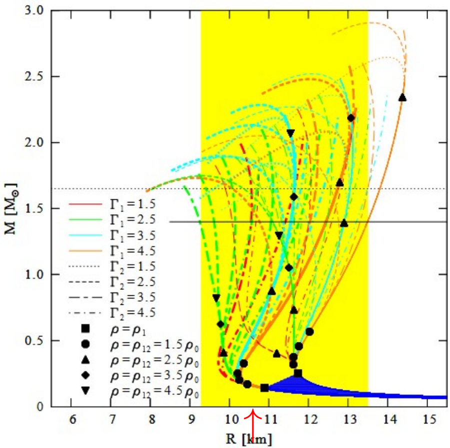

Hebeler, Lattimer & Schwenk 2010

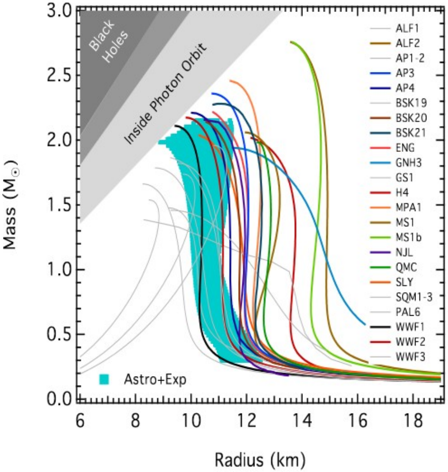

Özel & Freire 2016

Piecewise-Polytrope $R_{M=1.4}$ Distributions

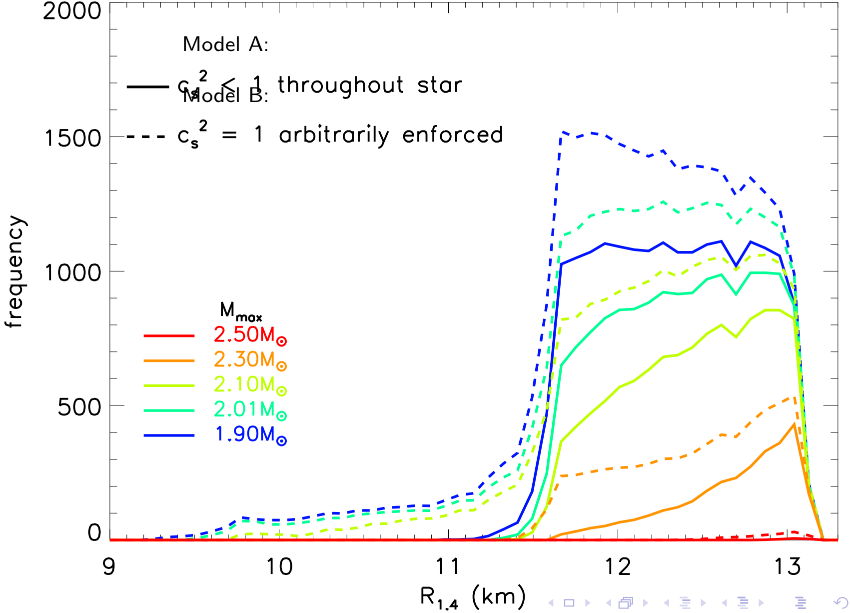

Piecewise-Polytrope Average Radius Distributions

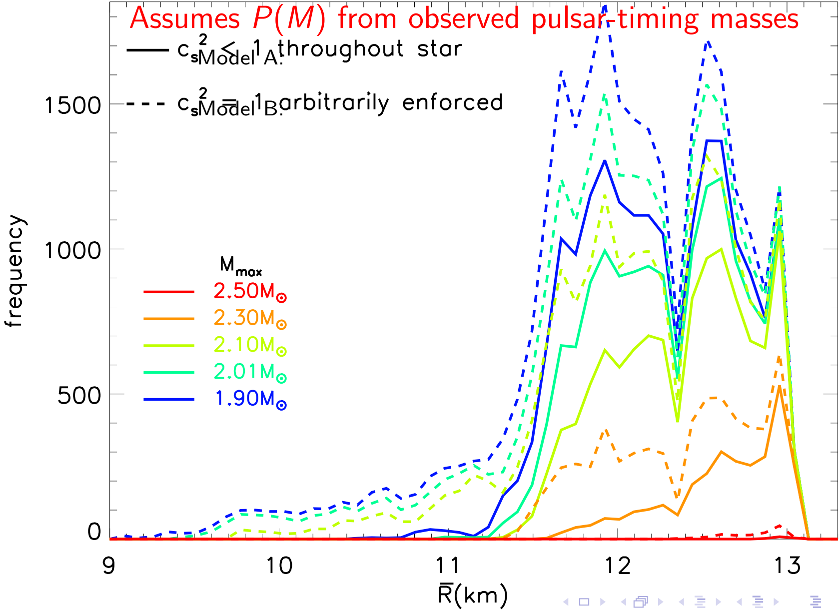

Universal Relations

With these assumptions

- Hadronic crust with well-known EOS
- Neutron matter constraint ($p_{min} < p_1 < p_{max}$)
- Two piecewise polytropes for $p > p_1$
- Causality is not violated
- M_{max} is limited from below from pulsar observations

model A yields interesting bounds to radius and tight correlations among the compactness, moment of inertia, binding energy and tidal deformability.

Moment of Inertia - Compactness Correlations

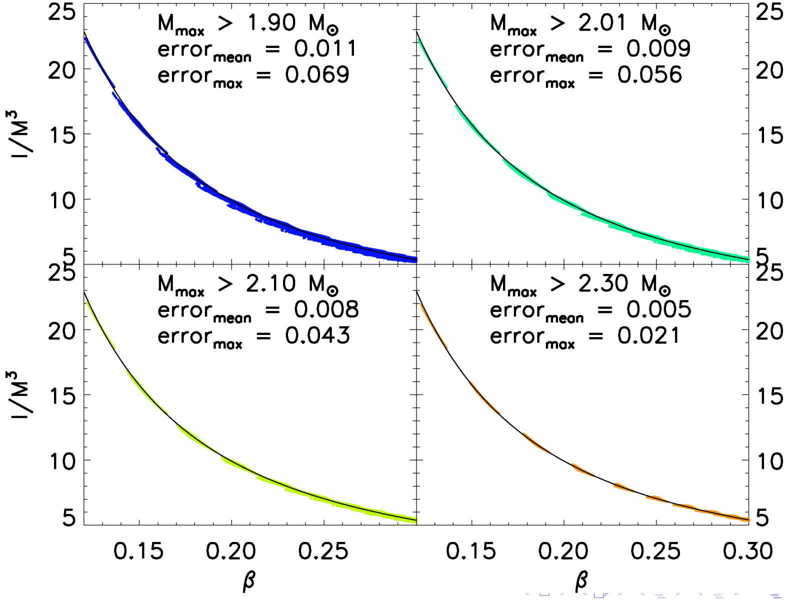

Moment of Inertia - Radius Constraints

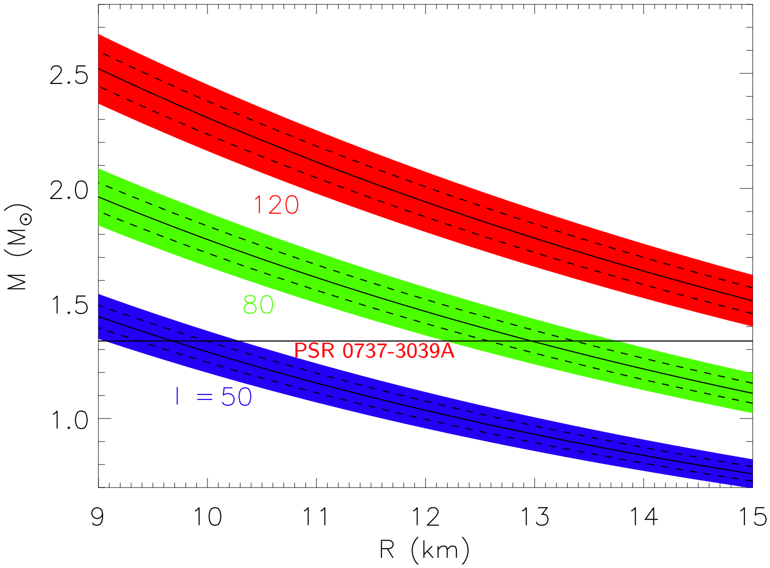

Binding Energy - Compactness Correlations

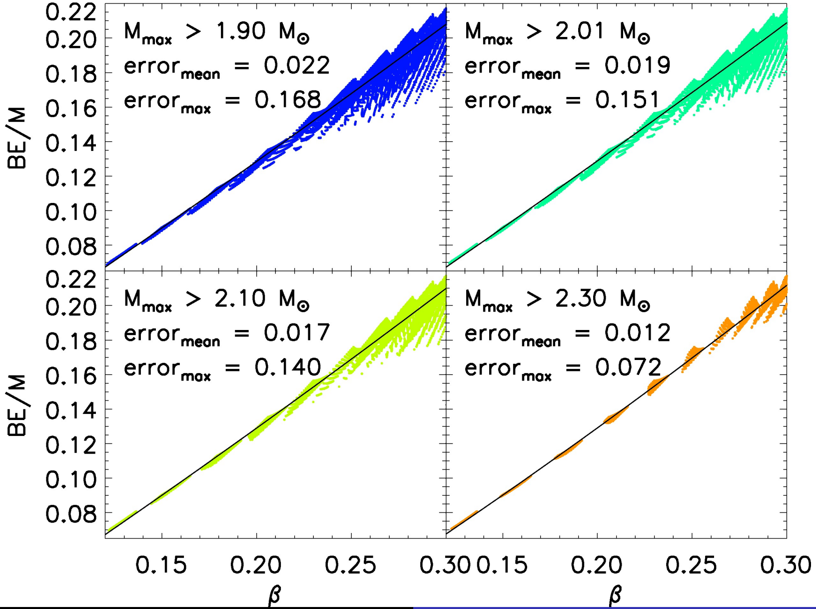

Binding Energy - Mass Correlations

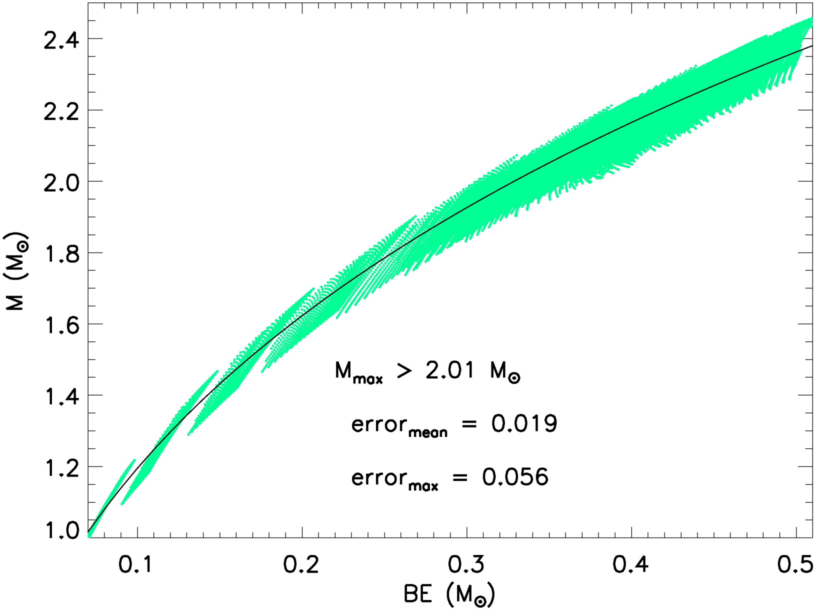

Tidal Deformatibility - Moment of Inertia

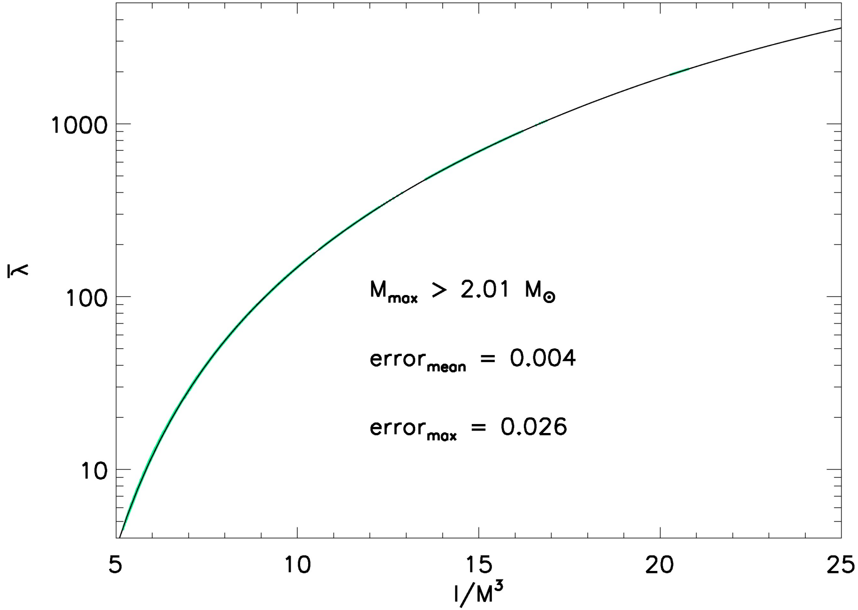

Tidal Deformability - Mass

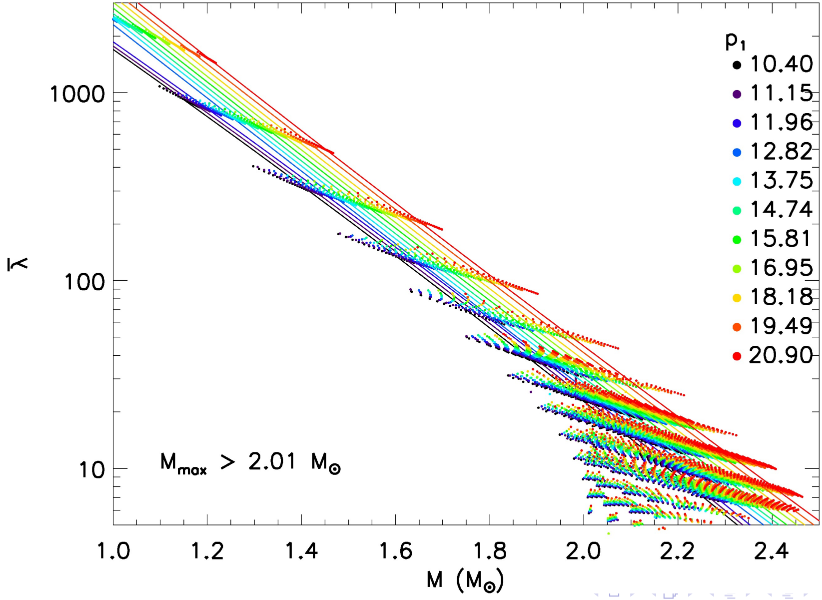

Tidal Deformatibility

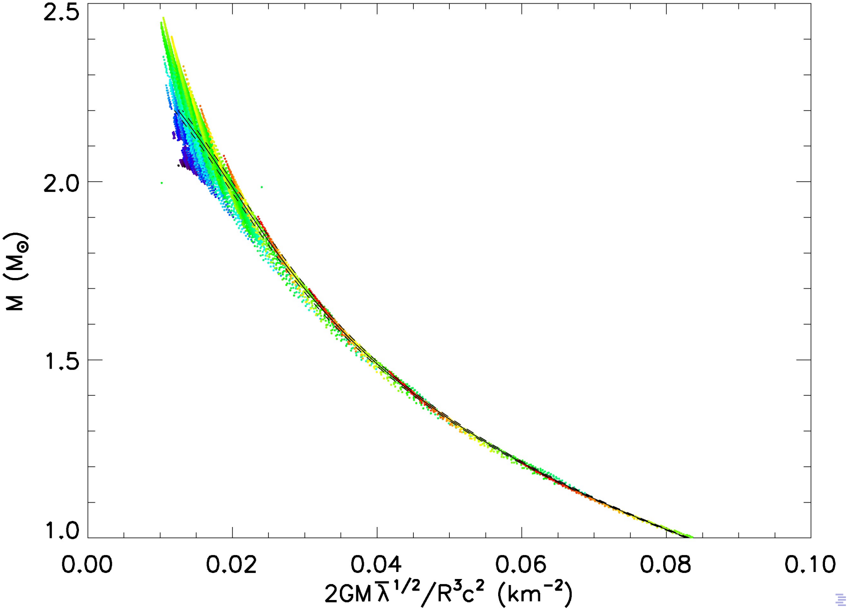

Tidal Deformability

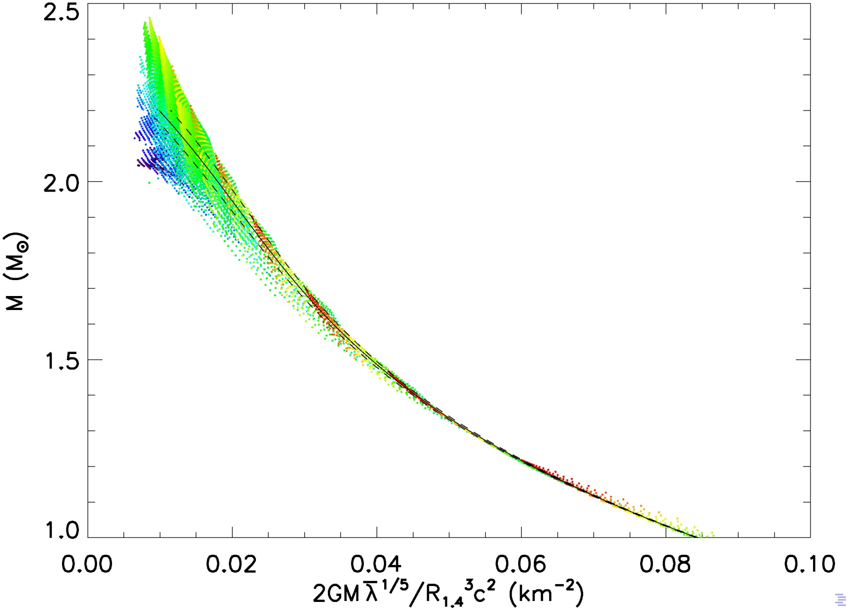

Binary Tidal Deformability

In a neutron star merger, both stars are tidally deformed. The most accurately measured deformability parameter is

$$\bar{\Lambda} = \frac{16}{13}\left[\bar{\lambda}_1 q^4(12q+1) + \bar{\lambda}_2(1+12q)\right]$$

where

$$q = \frac{M_1}{M_2} < 1$$

For $S/N \approx 20 - 30$, typical measurement accuracies are expected to be (Rodriguez et al. 2014; Wade et al. 2014):

$$\Delta M_{chirp} \sim 0.01 - 0.02\%, \qquad \Delta\bar{\Lambda} \sim 20 - 25\%$$

$$\Delta(M_1 + M_2) \sim 1 - 2\%, \qquad \Delta q \sim 10 - 15\%$$

Binary Tidal Deformatibility

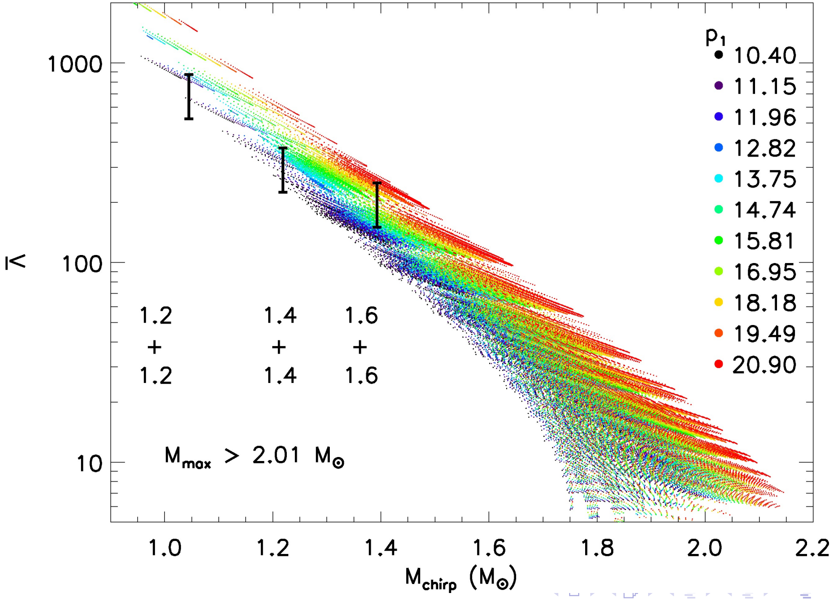

Binary Tidal Deformatibility

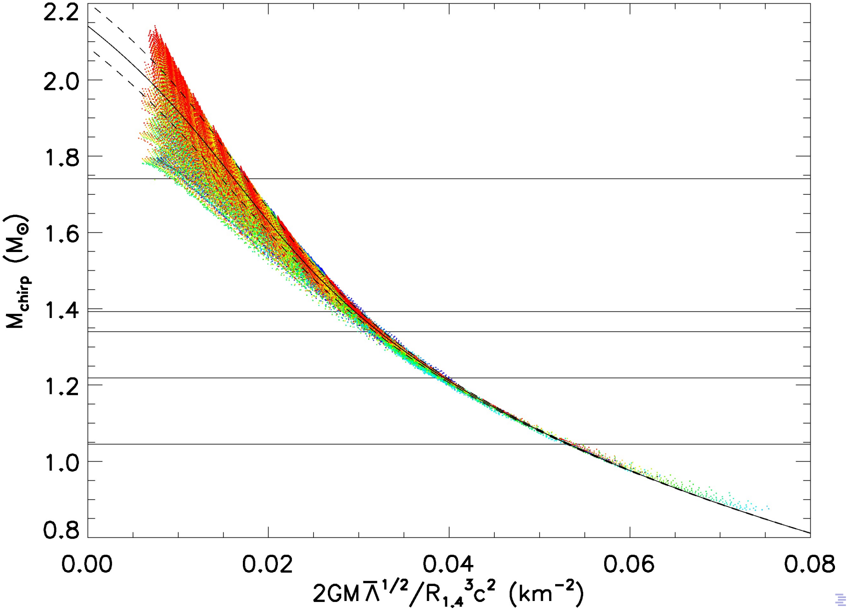

Binary Tidal Deformatibility

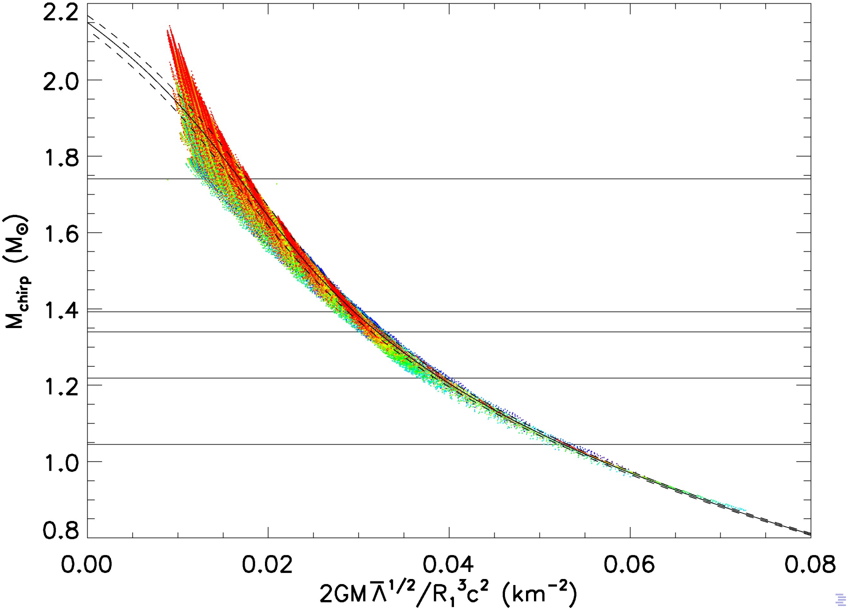

Simultaneous Mass/Radius Measurements

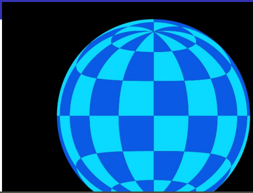

- Measurements of flux $F_\infty = (R_\infty/D)^2\,\sigma T_{\rm eff}^4$ and color temperature $T_c \propto \lambda_{\rm max}^{-1}$ yield an apparent angular size (pseudo-BB):

$$R_\infty/D = (R/D)/\sqrt{1-2GM/Rc^2}$$

- Observational uncertainties include distance D, interstellar absorption N_H, atmospheric composition

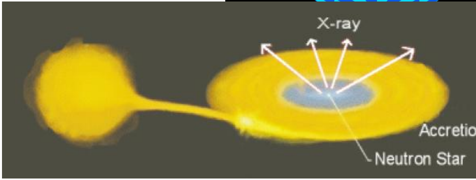

Best chances are:

  - Isolated neutron stars with parallax (atmosphere ??)
  - Quiescent low-mass X-ray binaries (QLMXBs) in globular clusters (reliable distances, low B H-atmospheres)
  - Bursting sources (XRBs) with peak fluxes close to Eddington limit (gravity balances radiation pressure)

$$F_{\rm Edd} = \frac{cGM}{\kappa D^2}\sqrt{1-2GM/Rc^2}$$

PRE Burst Models

Observational measurements:

$$F_{Edd,\infty} = \frac{GMc}{\kappa D}\sqrt{1-2\beta}, \qquad \beta = \frac{GM}{Rc^2}$$

$$A = \frac{F_\infty}{\sigma T_\infty^4} = f_c^{-4}\left(\frac{R_\infty}{D}\right)^2$$

Determine parameters:

$$\alpha = \frac{F_{Edd,\infty}}{\sqrt{A}}\frac{\kappa D}{f_c^4 c^3} = \beta(1-2\beta)$$

$$\gamma = \frac{A f_c^4 c^3}{\kappa F_{Edd,\infty}} = \frac{R_\infty}{\alpha}.$$

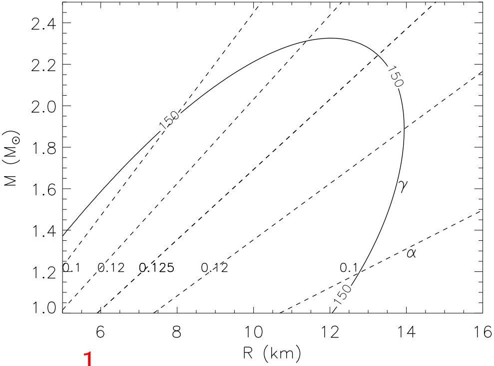

Solution:

$$\beta = \frac{1}{4} \pm \frac{\sqrt{1-8\alpha}}{4}, \qquad \alpha \leq \frac{1}{8} \text{ for real solutions.}$$

PRE $M - R$ Estimates

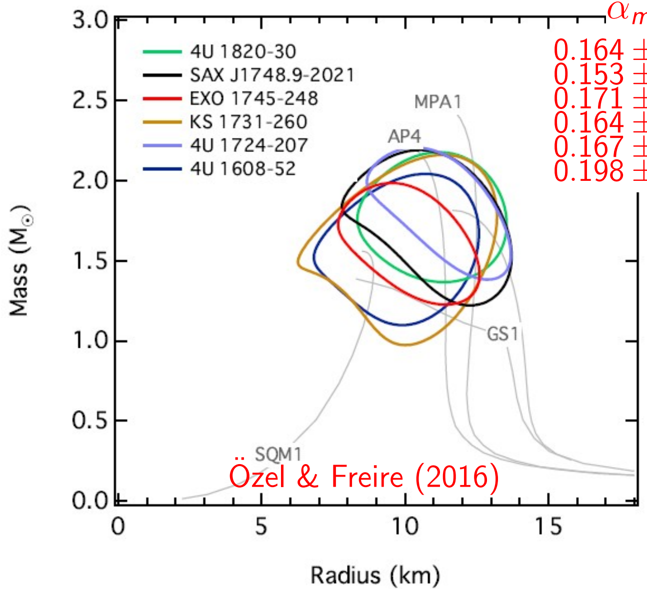

α_{min}

0.164 ± 0.024
0.153 ± 0.039
0.171 ± 0.042
0.164 ± 0.037
0.167 ± 0.045
0.198 ± 0.047

QLMXB $M - R$ Estimates

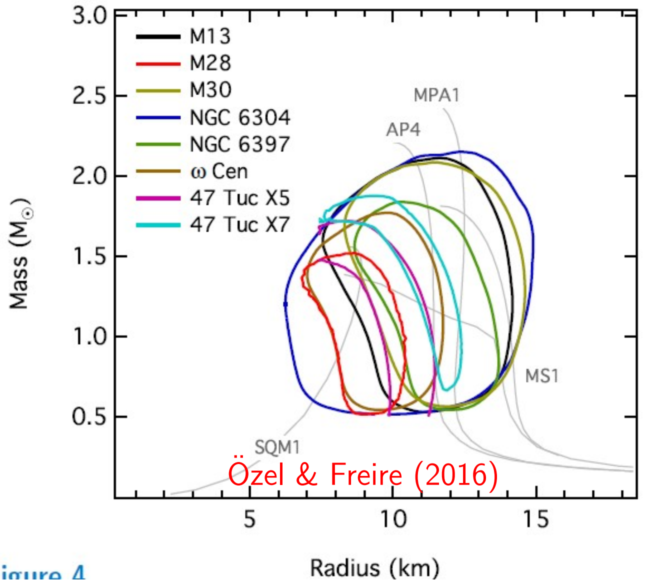

igure 4

Combined R fits

Assume $P(M)$ is that measured from pulsar timing ($\bar{M} = 1.4 M_\odot$).

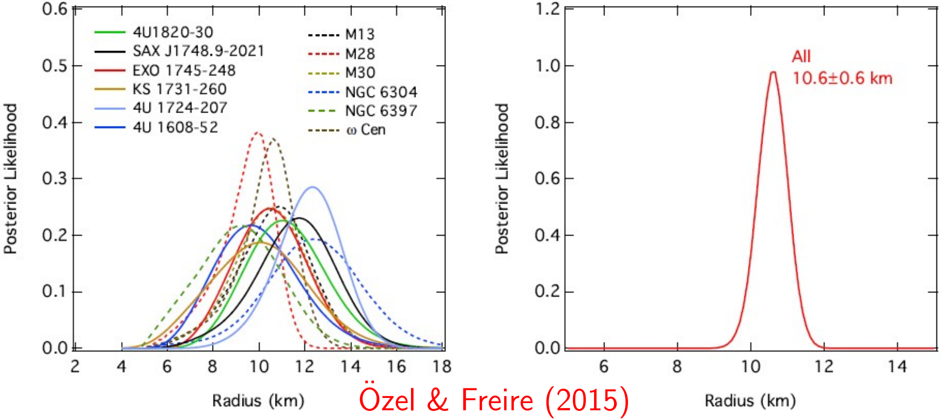

Özel & Freire (2015)

Folding Observations with Piecewise Polytropes

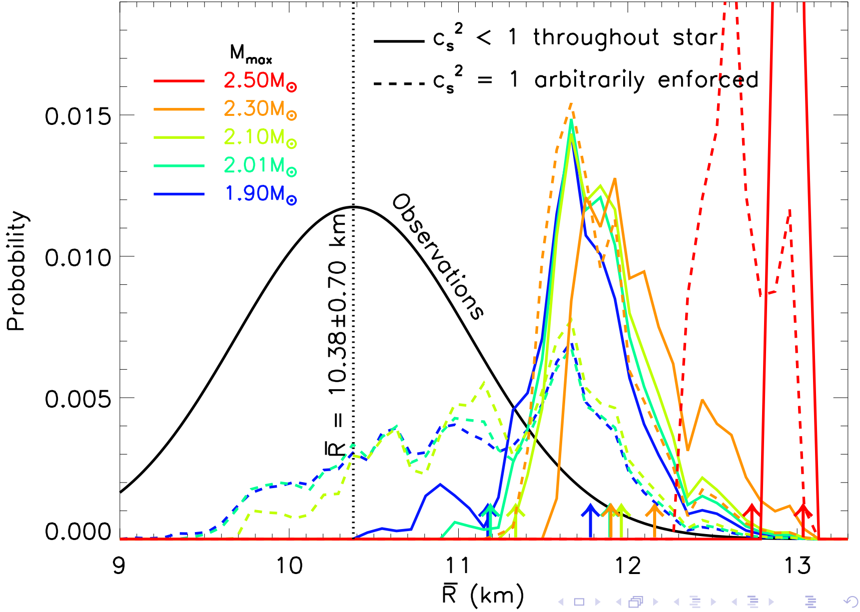

Bayesian Analyses

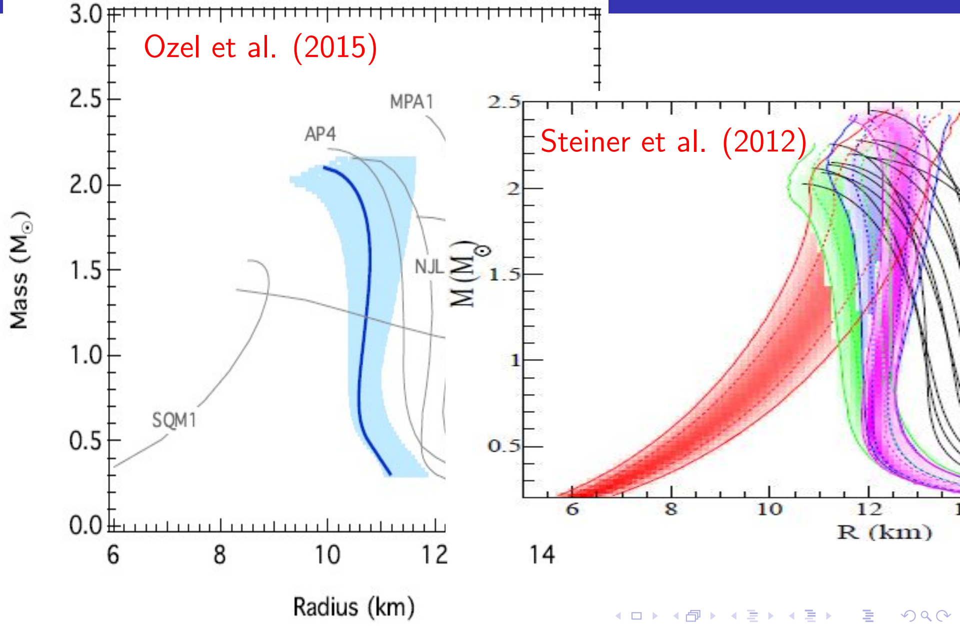

Role of Systematic Uncertainties

Systematic uncertainties plague radius measurements.

- Assuming uniform surface temperatures leads to underestimates in radii.
- Uncertainties in amounts of interstellar absorption
- Atmospheric composition: In quiescent sources, He or C atmospheres can produce about 50% larger radii than H atmospheres.
- Non-spherical geometries: In bursting sources, the use of the spherically-symmetric Eddington flux formula leads to underestimate of radii.
- Disc shadowing: In burst sources, leads to underprediction of $A = f_c^{-4}(R_\infty/D)^2$, overprediction of $\alpha \propto 1/\sqrt{A}$, and underprediction of $R_\infty \propto \sqrt{\alpha}$.

Additional Proposed Radius and Mass Constraints

- Pulse profiles Hot or cold regions on rotating neutron stars alter pulse shapes: NICER and LOFT will enable X-ray timing and spectroscopy of thermal and non-thermal emissions. Light curve modeling $\rightarrow M/R$; phase-resolved spectroscopy $\rightarrow R$.
- Moment of inertia Spin-orbit coupling of ultra- relativistic binary pulsars (e.g., PSR 0737+3039) vary i and contribute to $\dot{\omega}$: $I \propto MR^2$.
- Supernova neutrinos Millions of neutrinos detected from a Galactic supernova will measure BE$= m_B N - M$, $< E_\nu >$, τ_ν.
- QPOs from accreting sources ISCO and crustal oscillations

Neutron star Interior Composition ExploreR

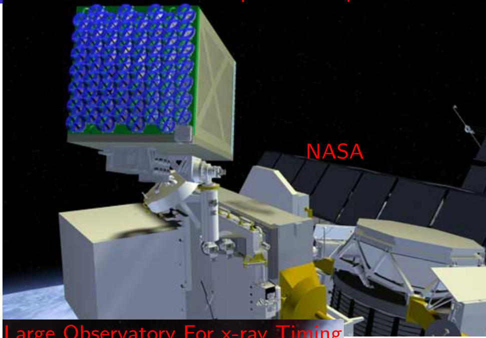

Large Observatory For x-ray Timing

Science Measurements

NICER

Reveal stellar structure through lightcurve modeling, long-term timing, and pulsation searches

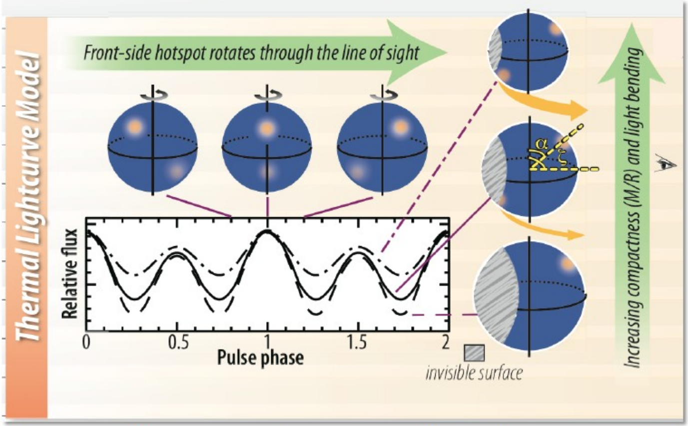

Lightcurve modeling constrains the compactness (M/R) and viewing geometry of a non-accreting millisecond pulsar through the depth of modulation and harmonic content of emission from rotating hot-spots, thanks to gravitational light-bending…

Science Measurements (cont.)

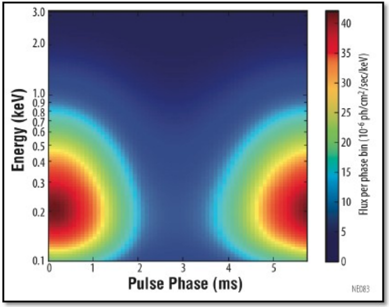

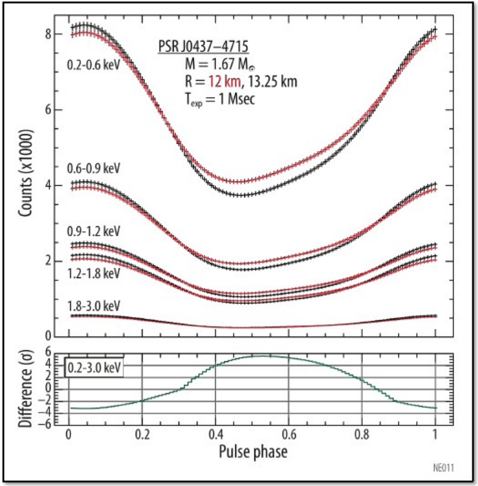

… while phase-resolved spectroscopy promises a direct constraint of radius R.

Conclusions

- Neutron matter calculations and nuclear experiments are consistent with each other and set reasonably tight constraints on symmetry energy behavior near the nuclear saturation density.
- These constraints, together with assumptions that neutron stars have hadronic crusts and are causal, predict neutron star radii $R_{1.4}$ in the range 12.0 ± 1.0 km.
- Astronomical observations of photospheric radius expansion X-ray bursts and quiescent sources in globular clusters suggest $R_{1.4} \sim 10.5 \pm 1$ km, unless maximum mass and EOS priors are implemented.
- Should observations require smaller or larger neutron star radii, a strong phase transition in extremely neutron-rich matter just above the nuclear saturation density is suggested. Or should GR be modified?